Kinetic Modelling of Synaptic Functions in the Alpha Rhythm Neural Mass Model

Basabdatta Sen Bhattacharya[1], Damien Coyle[2], Liam P. Maguire[2], and Jill Stewart[1]

[1] University of Lincoln, Lincoln, UK
[2] University of Ulster, Northern Ireland, UK

Abstract. In this work, we introduce the kinetic framework for modelling synaptic transmission in an existing neural mass model of the thalamocortical circuitry to study Electroencephalogram (EEG) slowing within the alpha frequency band (8–13 Hz), a hallmark of Alzheimer's disease (AD). Ligand-gated excitatory and inhibitory synapses mediated by AMPA (α-amino-3-hydroxy-5-methyl-4-isoxazolepropionic acid) and $GABA_A$ (gamma-amino-butyric acid) receptors respectively are modelled. Our results show that the concentration of the GABA neurotransmitter acts as a bifurcation parameter, causing the model to switch from a limit cycle mode to a steady state. Further, the retino-geniculate pathway connectivity plays a significant role in modulating the power within the alpha band, thus conforming to research proposing ocular biomarkers in AD. Overall, kinetic modelling of synaptic transmission in neural mass models has enabled a more detailed investigation into the neural correlates underlying abnormal EEG in AD.

1 Introduction

EEG-based longitudinal studies in Alzheimer's Disease (AD) provide evidence of a definite 'slowing' (decrease in the peak frequency of oscillation) within the alpha(8–13 Hz) frequency band [1]. The Alpha Rhythm model (ARm) is a seminal work by Lopes da Silva in implementing neural mass models to generate alpha rhythms when the input is a Gaussian white noise [2], and has been the basis of our research in investigating alpha rhythm slowing in AD [3]. Subsequently, we have modified the ARm based on recent experimental findings [4]. Our results have shown that the synaptic connectivity in the inhibitory pathway of the thalamocortical model play a significant role in modulating the alpha frequency slowing in the model output. However, deficiency in synaptic pathways such as seen in AD may also arise from other factors during synaptic transmission, for example neurotransmitter concentration in the synaptic cleft, which is known to play a vital role in brain oscillatory activity [5]. Current framework for neural mass models use an exponential function (commonly known as Ralls alpha function [6]) to mimic the synaptic dynamics as a function of time. While this is a fair estimate of the overall synaptic function [7], the details of neurotransmitter dynamics are ignored. To address this issue, we propose implementing 'kinetic

A.E.P. Villa et al. (Eds.): ICANN 2012, Part I, LNCS 7552, pp. 645–652, 2012.

models' of synaptic functions [8][9] within the neural mass modelling framework as an alternative to Rall's alpha function.

Kinetic models have been proposed in [8][9] as a more biologically plausible manner of modelling the dynamics of synaptic transmission involving the Glutamatergic and GABA (gamma-amino-butyric acid)-ergic neurotransmitters. However, the implementation of these models in the neural mass modelling paradigm have not been explored; thus, synaptic activities prior to the post-synaptic-potential (PSP), for example post-synaptic current (PSC), receptor dynamics, etc. are ignored. More recently, Suffczyński et al [10] have introduced an integrator in their neural mass model to implement the rate change of the PSP as a direct proportion to the sum of the PSCs, an approach that is commonly used in the single neuronal modelling paradigm. Implementing such an approach [10], we use kinetic models of synaptic transmission in the modified ARm as presented in [4]. Each parameter in the kinetic model is assumed to be an 'ensemble representation' of the respective cell population i.e., the neural mass. Our results indicate that firstly, the steepness of the neurotransmitter concentration function in the inhibitory pathway plays a vital role in modulating the output time-series plots; secondly, the retino-geniculate pathway connectivity parameter plays an important role in modulating the dominant frequency within the alpha band and in spite of a very low relative parameter value, which supports research proposing ocular biomarkers in AD. [11].

In Section 2, we describe the ARm while using the kinetic modelling framework. In Section 3 we mention the empirical methods and results. We conclude this paper in Section 4.

2 The Alpha Rhythm Model: Introducing the Kinetic Framework

The kinetic framework for modelling neurotransmitter-based synaptic transmission was first proposed in [8], where the parameterisation was based on experimental data from the hippocampus. About the same time, a similar approach was adopted in [12][13] to mimic neurotransmitter dynamics informed by in-vitro studies on rodent thalamic slices. Recently, these parameters were used by Suffczyński et al in their neural mass model of the thalamocortical circuitry [10]. In this work, we adopt the kinetic framework as in [8] and parameterise the synaptic functions as in [10][13].

The Alpha Rhythm model (ARm) has an excitatory cell population representing the thalamocortical relay cells (TCR) of the Lateral Geniculate Nucleus (LGN—the thalamic nuclei in the visual pathway), and an inhibitory cell population representing the interneurons (IN); the synaptic connectivity layout and parameterisation in the model was based on Tombol's (1967) experimental studies. Newer studies on cat and rat thalamus have revealed a lack of consensus on the feedback pathway from the IN to the TCR cell population [14]. Moreover, the connectivities between the TCR cells and those of the Thalamic Reticular Nucleus (TRN) are now known to play a vital role in brain oscillations [15]. Thus,

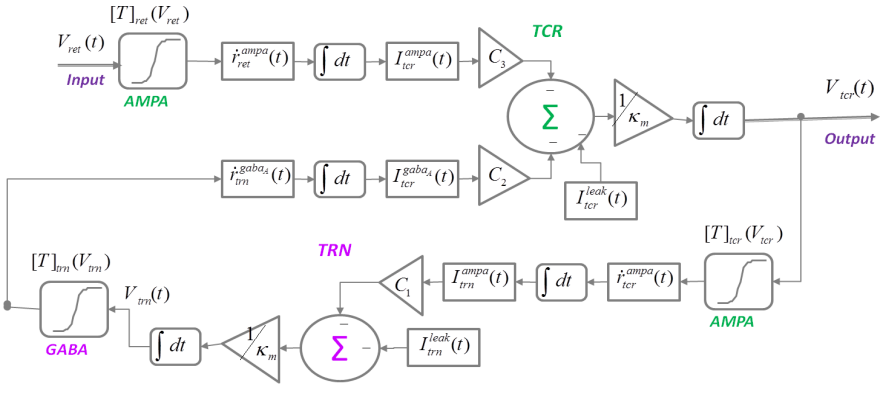

Fig. 1. The kinetic modelling framework introduced in the modified Alpha Rhythm model proposed in [4]. The input (V_{ret}) to the model is assumed to be from the retinal cells ('ret'), while the output of the model (V_{tcr}) is the membrane potential of the thalamocortical relay (TCR) cells. The excitatory and inhibitory synapses in the model are mediated by AMPA (α-amino-3-hydroxy-5-methyl-4-isoxazolepropionic acid) and $GABA_A$ (gamma-amino-butyric acid) receptors respectively. All parameters are assumed to be an 'ensemble representation' corresponding to a pre-synaptic ($\bar{\chi} \in \{ret, tcr, trn\}$) and post-synaptic ($\bar{\Upsilon} \in \{tcr, trn\}$) cell population and are defined in Equations 1–5. The parameter values are defined in Table 1.

in subsequent works [16] as well as in our previous research [4], the inhibitory cell population in the ARm is assumed to be those of the TRN; we follow the same in this work.

The modified ARm (as in [4]) with the kinetic framework for modelling synaptic functions is shown in Fig. 1. The input to the model is assumed to be the collective membrane potential of the pre-synaptic neuronal population. Since the model is based on information obtained through experimental studies on the visual pathway (retina-LGN-visual cortex), the sensory input is assumed to be that from the retinal cells (V_{ret}). Moreover, brain alpha rhythms are most prominent in EEG from the occipital lobe (seat of the visual cortex) under conditions of relaxed wakefulness and with eyes closed. This can be thought to be a resting state with no sensory input and is simulated using a Gaussian white noise [2] with a mean μ and standard deviation φ. The excitatory synapses made by the TCR cell population involves glutamate (an amino-acid) as the neurotransmitter; the inhibitory synapses by the TRN population are facilitated by the neurotransmitter gamma-amino-butyric-acid (GABA). The receptors to these neurotransmitters may either be ligand-gated (i.e. they bind to the neurotransmitters to initiate the opening of an ion channel on the post-synaptic membrane) or second-messenger-gated (i.e. they bind to the neurotransmitter to trigger another protein molecule, referred to as the 'second-messenger', to initiate the opening of an ion channel). The glutamatergic synapses from the retina to the TCR activate the ligand-gated AMPA (α-amino-3-hydroxy-5-methyl-4-isoxazolepropionic acid) receptors. For brevity in this work, we consider

ligand-gated AMPA receptors (and ignore other types of glutamatergic receptors) for synapses from the TCR cell population to the TRN cell population. The GABA-ergic synapses by the TRN on the TCR involves both ligand-gated ($GABA_A$) and secondary-messenger-gated ($GABA_B$) synapses. Again, for brevity, we consider synapses involving the $GABA_A$ receptors only.

All variables presented in the equations below are assumed to be the 'ensemble representation' corresponding to a neural mass. The concentration of neurotransmitters in the synaptic cleft ($[T]_{\bar{\chi}}$) is defined as a function of the pre-synaptic membrane potential $V_{\bar{\chi}}(t)$, where $\bar{\chi} \in \{ret, tcr, trn\}$ refers to the pre-synaptic neuronal population, and is expressed as a sigmoid function defined in Eq. (1).

$$[T]_{\bar{\chi}}(V_{\bar{\chi}}(t)) = \frac{T_{max}}{1 + exp\,(-\frac{V_{\bar{\chi}}(t) - \theta_s}{\sigma_s})} \tag{1}$$

T_{max} is the maximum neurotransmitter concentration and is well approximated by 1 mM (milli Mole) [8]. The parameter θ_s represents the threshold at which $[T]_{\bar{\chi}} = 0.5T_{max}$ while σ_s denote the steepness of the sigmoid. The proportion of open ion-channels on the ensemble membrane of the post-synaptic cell population corresponding to the synapse made by the pre-synaptic population $\bar{\chi}$ mediated by the receptor $\bar{\eta}$, where $\bar{\eta} \in \{AMPA, GABA_A\}$ is defined in Eq. (2):

$$\frac{dr_{\bar{\chi}}^{\bar{\eta}}(t)}{dt} = \alpha_{\bar{\eta}}[T]_{\bar{\chi}}(1 - r_{\bar{\chi}}^{\bar{\eta}}(t)) - \beta_{\bar{\eta}} r_{\bar{\chi}}^{\bar{\eta}}(t) \tag{2}$$

where $\alpha_{\bar{\eta}}$ and $\beta_{\bar{\eta}}$ are the rate transitions from the open to the closed state and vice-versa respectively. The resulting change in the ensemble PSC is defined in Eq. (3):

$$I_{\bar{\chi}}^{\bar{\eta}}(t) = g_{\bar{\eta}} r_{\bar{\chi}}^{\bar{\eta}}(t)(V_{\bar{\Upsilon}}(t) - V_{\bar{\eta}}) \tag{3}$$

where $g_{\bar{\eta}}$ and $V_{\bar{\eta}}$ are the maximum conductance and reverse potential, respectively, of the ensemble membrane of the post-synaptic cell population corresponding to the $\bar{\eta}$ mediated synapse; $V_{\bar{\Upsilon}}(t)$ is the ensemble membrane potential of the post synaptic cell population $\bar{\Upsilon} = \{tcr, trn\}$ defined in Eq. (4):

$$\kappa_m \frac{V_{\bar{\Upsilon}}(t)}{dt} = - \sum_{\bar{\chi} \in \{ret, tcr, trn\}} I_{\bar{\chi}}^{\bar{\eta}}(t).C_n - I_{\bar{\Upsilon}}^{leak}(t), \tag{4}$$

where κ_m is the ensemble capacitance of the post-synaptic cell population; C_n, $n \in \{1, 2, 3\}$, is the synaptic connectivity expressed as a percentage of the total number of synaptic contacts made by a pre-synaptic population on the post-synaptic population and is based on experimental data obtained from the cat and rat thalamus [14][17]; $I_{\bar{\Upsilon}}^{leak}$ is the ensemble leak current of the post-synaptic membrane and is defined in Eq. (5):

$$I_{\bar{\Upsilon}}^{leak}(t) = g_{\bar{\Upsilon}}^{leak}(V_{\bar{\Upsilon}}(t) - V_{\bar{\Upsilon}}^{leak}), \tag{5}$$

where $g_{\bar{\Upsilon}}^{leak}$ and $V_{\bar{\Upsilon}}^{leak}$ are conductance and reverse potential, respectively, corresponding to 'non-specific' leak [13][10] in the ensemble membrane of the post synaptic cell population. All parameter values defined in Equations (1)–(5) are mentioned in Table 1.

Table 1. Values of the parameters defined in Equations (1)–(5)

$[T]_{\bar{\chi}}$ (mV)		C_n (Percentage)			$\alpha_{\bar{\eta}}$ $(mM.msec)^{-1}$		$\beta_{\bar{\eta}}$ $(msec^{-1})$		$g_{\bar{\eta}}$ (mS)		$V_{\bar{\eta}}$ (mV)		$g_{\bar{\Upsilon}}^{leak}$ (mS)		$V_{\bar{\Upsilon}}^{leak}$ (mV)	
θ_s	σ_s	C_1	C_2	C_3	ampa	$gaba_A$	ampa	$gaba_A$	ampa	$gaba_A$	ampa	$gaba_A$	tcr	trn	tcr	trn
-40	4	30	24	7	2	2	0.1	0.08	0.1	0.2	0	-75	0.02	0.025	-65	-70

3 Empirical Methods and Results

All differential equations are solved using the Euler's method in Matlab. The total simulation time is 300 seconds (5 minutes) with a resolution of 1 msec. Initial value of all $r_{\bar{\eta}}$ defined in Eq. (2) is 0.0002. The initial values of V_{tcr} and V_{trn} (resting state membrane potential of excitatory and inhibitory cell populations respectively) are -55 mV and -70mV respectively [10] [13]. V_{ret} is simulated by a Gaussian white noise with mean μ =-55 mV, (as we consider resting state firing activity of the retinal cells) and a standard deviation φ =20mV. The value of the standard deviation is chosen by trial and error so that the function $[T]_{ret}(V_{ret})$ covers all region of the sigmoid and is shown in Fig. 2(a) for varying values of the steepness parameter σ_s. The output voltage time series is averaged over 50 trials, each with a different seed for the noisy input. For frequency analysis, an epoch of the output signal from 20–290 seconds is extracted and sampled every 2 msec (500 Hz). A Butterworth filter of order 10 is used to bandpass the signal within 0.5 and 50 Hz. The power spectral density is obtained using a Welch's periodogram with a Hamming window of segment length $\frac{1}{2}$ the size of the sampling frequency and overlap of 50% [18].

First we vary the parameters in Eq. (1) to study the effects of neurotransmitter concentration on the model output V_{tcr}. We observe that the steepness parameter σ_s has a significant effect on the model behaviour. The (ascending) 'ordered' values of $[T]_{trn}$ in Fig. 2(b) shows a clear bifurcation in behaviour for $\sigma_s > 3$ when all values of $[T]_{trn}$ are ≈ 1. The time-series plots for $[T]_{trn}$ for $\sigma_s \leqslant 3$ are shown in Figures 2(c)–2(e). An antiphase behaviour is seen in similar plots for V_{tcr} (Figures 2(f)–2(i)) and $[T]_{tcr}$ (Figures 2(j)–2(m)) for values of $\sigma_s \leqslant 3$; for $\sigma_s > 3$ (Figures 2(i), 2(m)), the noisy pattern of the input emerges and V_{tcr} and $[T]_{tcr}$ fluctuate within small ranges of $\approx 10\mu V$ and $\approx 1\mu M$ respectively. Thus, we may say that for $\sigma_s > 3$, $[T]_{trn}$ switches from a sigmoid to a minimally fluctuating plot around its maximum value of 1 mM, which causes the model output to come out from the limit cycle mode and settle into a noisy pattern around a stable mean value.

Second, we vary the connectivity parameters C_1, C_2 and C_3 in the model and observe the change in power at each of 8–13 Hz i.e. frequencies within the alpha band of EEG oscillation. In Fig. 3, we observe that the model oscillates with a dominant frequency within 8 Hz with all parameter values at their base values as defined in Table 1. Figure 3(a) shows a slight increase in power at 8, 9 and 10 Hz with increasing values of C_1; there is a slight decrease in power at 12 Hz, while at 13 Hz, there is no visible change in power. Thus, we may say that there is a

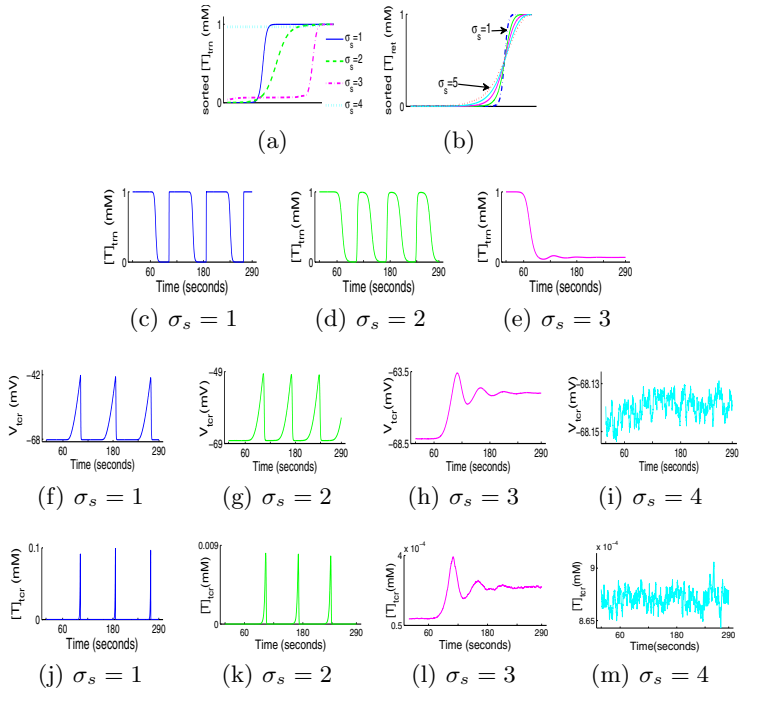

Fig. 2. Plots of the neurotransmitter concentration due to synaptic activity by the (a) TRN and (b) retinal cell populations sorted in an ascending order. The time-series plots of: the neurotransmitter concentration due to synaptic activity by the (c)–(e) TRN and (j)–(m) the TCR cell populations; (f)–(i) the model output V_{tcr} with varying σ_s in Eq. (1).

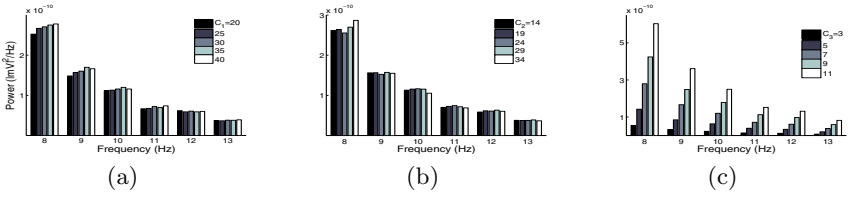

Fig. 3. Power within the alpha frequency band (8–13 Hz) with varying values (see figure legends) of the connectivity parameters (a) C_1 (b) C_2 and (c) C_3

slowing in alpha rhythm, where power within the lower frequency bands increase, while that in the upper frequency bands either decrease or do not change. The plot for C_2 in Fig. 3(b) show a similar slowing. On the other hand, a significant variation in power at all frequencies within the alpha band is seen with varying values of C_3 in Fig. 3(c); this in spite that C_3 is only a small percentage of the total synapses relative to C_1 and C_2. This supports research suggesting possible role of visual circuitry towards providing biomarkers in AD [11].

4 Conclusion

We have introduced the kinetic framework of modelling synaptic transmission in a simple neural mass model of the thalamocortical circuitry (Fig. 1). We have considered AMPA-mediated synapses in the excitatory input (retinal to TCR) and feed-forward (TCR to TRN) pathways, and $GABA_A$-mediated synapses in the inhibitory feedback (TRN to TCR) pathway. The receptor dynamics are implemented using the kinetic framework proposed in [8], while model parameterisation is done as in [10][13]. Our results show that first, the steepness of the neurotransmitter concentration function acts as a critical parameter and significantly affects the inhibitory neurotransmitter concentration, which in turn effects an oscillatory model output. With progressive increase in the steepness parameter, the inhibitory neurotransmitter concentration transforms from a sigmoidal shape to an 'on'-state whereby it is always within 10% of its maximum value. This effects a 'gating mechanism', whereby the model bifurcates from the limit-cycle mode to a steady state signal over-ridden by a noisy pattern reflecting the noisy input to the model. Limit cycle oscillation during awake state is generally associated with neurological disorders. Thus, the results suggest that a fall in the level of inhibitory neurotransmitter concentration in the synaptic cleft leads to abnormal brain oscillations, which conform to reports about the vital role of the TRN in modulating thalamocortical oscillatory activity [14].

Second, we observe a significant role of the retino-geniculate connectivity in modulating the power within the alpha band, which conform to recent research suggesting the role of the visual circuitry in AD [11]. Overall, we observe that introducing kinetic models of synaptic transmission has enabled a more detailed investigation into the neural correlates of abnormal EEG in AD.

However, this is a preliminary study on a simple model. Furthermore, the slowing of alpha rhythm with increased synaptic connectivity in the model are not in agreement with experimental results proposed in [19][20], which indicate a decrease in both excitatory and inhibitory connectivity in AD. We speculate that a more biologically plausible thalamocortical model structure (for example as in [18]) may produce results that will provide greater support to experimental findings; we propose this as a future work.

References

1. Soininen, H., Reinikainen, K., Partanen, J., Helkala, E.L., Palijarvi, L., Riekkinen, P.: Slowing of Electroencephalogram and Choline Acetyltransferase Activity in Post Mortem Frontal Cortex in Definite Alzheimer's Disease. Neurosc. 49, 529–535 (1992)
2. da Silva, F.H.L., Hoeks, A., Smits, H., Zetterberg, L.H.: Model of Brain Rhythmic Activity. Kybernetic 15, 23–37 (1974)
3. Sen Bhattacharya, B., Coyle, D., Maguire, L.P.: Thalamocortical Circuitry and Alpha Rhythm Slowing: an Empirical Study Based on a Classic Computational Model. In: IEEE Proceedings of the IJCNN, Barcelona, pp. 3912–3918 (2010)

4. Sen Bhattacharya, B., Coyle, D., Maguire, L.P.: Alpha and theta rhythm abnormality in Alzheimer's Disease: a study using a computational model. In: Hernández, C., Gómez, J., Sanz, R., Alexander, I., Smith, L., Hussain, A., Chella, A. (eds.) Advances in Experimental Medicine and Biology: From Brains to Systems, vol. 718, pp. 57–73. Springer, New York (2011)
5. Basar, E., Guntekin, B.: A review of brain oscillations in cognitive disorders and the role of neurotransmitters. Br. Res. Rev. 1235, 172–193 (2008)
6. Rall, W.: Distinguishing Theoretical Synaptic Potentials Computed for Different Soma-Dendritic Distributions of Synaptic Inputs. J. Neurophysiol. 30, 1138–1168 (1967)
7. Bernard, C., Ge, Y.C., Stockley, E., Willis, J.B., Wheal, H.V.: Synaptic Integration of NMDA and Non-NMDA Receptors in Large Neuronal Network Models Solved by Means of Differential Equations. Biol. Cybern. 70, 267–273 (1994)
8. Destexhe, A., Mainen, Z.F.: Synthesis of Models for Excitable Membranes, Synaptic Transmission and Neuromodulation Using A Common Formalism. J. Comp. Neurosc. 1, 195–230 (1994)
9. Destexhe, A., Mainen, Z.F., Sejnowski, T.J.: An Efficient Method for Computing Synaptic Conductances Based on a Kinetic Model of Receptor Binding. Neural Comp. 6, 14–18 (1994)
10. Suffczyński, P., Kalitzin, S., da Silva, F.H.L.: Dynamics of Non-convulsive Epileptic Phenomena Modelled by a Bistable Neuronal Network. Neurosc. 126, 467–484 (2004)
11. Frost, S., Martins, R.N., Kanagasingam, Y.: Ocular biomarkers for early detection of Alzheimer's Disease. J. Alzheimer's Disease 22(1), 1–16 (2010)
12. Wang, X., Golomb, D., Rinzel, J.: Emergent Spindle Oscillations and Intermittent Burst Firing in a Thalamic model: Specific Neuronal Mechanisms. PNAS 92, 5577–5581 (1995)
13. Golomb, D., Wang, X., Rinzel, J.: Propagation of Spindle Waves in a Thalamic Slice Model. J. Neurophysiol. 75, 750–769 (1996)
14. Sherman, S.M., Guillery, R.W.: Exploring the Thalamus and its Role in Cortical Functioning. Academic Press, New York (2006)
15. van Krosigk, M., Bal, T., McCormick, D.A.: Cellular Mechanisms of a Synchronized Oscillation in the Thalamus. Science 261, 361–364 (1993)
16. Suffczyński, P.: Neural Dynamics Underlying Brain Thalamic Oscillations Investigated with Computational Models. Ph.D. Dissertation, Institute of Experimental Physics, University of Warsaw (2000)
17. Horn, S.C.V., Erisir, A., Sherman, S.M.: Relative Distribution of Synapses in the A-laminae of the Lateral Geniculate Nucleus of the Cat. J. Compar. Neurol. 416, 509–520 (2000)
18. Sen Bhattacharya, B., Coyle, D., Maguire, L.P.: A Thalamo-Cortico-Thalamic Neural Mass Model To Study Alpha Rhythms in Alzheimer's Disease. Neur. Netw. 24, 631–635 (2011)
19. Satoh, J., Tabira, T., Sano, M., Nakayama, H., Tateishi, J.: Parvalbumin-immunoreactive Neurons in the Human Central Nervous System are Decreased in Alzheimer's Disease. Acta Neuropathol. 81(4), 388–395 (1991)
20. Braak, H., Braak, E.: Alzheimer's Disease Affects Limbic Nuclei of the Thalamus. Acta Neuropathol. 81(3), 261–268 (1991)